Anticodon Recognition and Discrimination by the α-Helix Cage Domain of Class I Lysyl-tRNA Synthetase †

ARTICLE *in* BIOCHEMISTRY · NOVEMBER 2007

Impact Factor: 3.02 · DOI: 10.1021/bi700815a · Source: PubMed

6 AUTHORS, INCLUDING:

Dieter Soll
Yale University
549 PUBLICATIONS **20,092** CITATIONS
SEE PROFILE

Michael Ibba
The Ohio State University
164 PUBLICATIONS **5,486** CITATIONS
SEE PROFILE

Published in final edited form as:
Biochemistry. 2007 October 2; 46(39): 11033–11038. doi:10.1021/bi700815a.

Anticodon Recognition and Discrimination by the α-Helix Cage Domain of Class I Lysyl-tRNA Synthetase[†]

Jeffrey D. Levengood[‡], **Hervé Roy**[§], **Ryuichiro Ishitani**[‖], **Dieter Söll**[⊥], **Osamu Nureki**[‖], and **Michael Ibba**[*,‡,§]

Ohio State Biochemistry Program and Department of Microbiology, The Ohio State University, Columbus, Ohio 43210, Department of Biological Information, Graduate School of Bioscience and Biotechnology, Tokyo Institute of Technology, Tokyo, Japan, and Department of Molecular Biophysics and Biochemistry, Yale University, New Haven, Connecticut 06511

Abstract

Aminoacyl-tRNA synthetases are normally found in one of two mutually exclusive structural classes, the only known exception being lysyl-tRNA synthetase which exists in both classes I (LysRS1) and II (LysRS2). Differences in tRNA acceptor stem recognition between LysRS1 and LysRS2 do not drastically impact cellular aminoacylation levels, focusing attention on the mechanism of tRNA anticodon recognition by LysRS1. On the basis of structure-based sequence alignments, seven $tRNA^{Lys}$ anticodon variants and seven LysRS1 anticodon binding site variants were selected for analysis of the *Pyrococcus horikoshii* LysRS1–$tRNA^{Lys}$ docking model. LysRS1 specifically recognized the bases at positions 35 and 36, but not that at position 34. Aromatic residues form stacking interactions with U34 and U35, and aminoacylation kinetics also identified direct interactions between Arg502 and both U35 and U36. Tyr491 was also found to interact with U36, and the Y491E variant exhibited significant improvement compared to the wild type in aminoacylation of a $tRNA^{Lys}_{UUG}$ mutant. Refinement of the LysRS1–$tRNA^{Lys}$ docking model based upon these data suggested that anticodon recognition by LysRS1 relies on considerably fewer interactions than that by LysRS2, providing a structural basis for the more significant role of the anticodon in tRNA recognition by the class II enzyme. To date, only glutamyl-tRNA synthetase (GluRS) has been found to contain an α-helix cage anticodon binding domain homologous to that of LysRS1, and these data now suggest that specificity for the anticodon of $tRNA^{Lys}$ could have been acquired through relatively few changes to the corresponding domain of an ancestral GluRS enzyme.

Translation, central to all living cells, is the process of synthesizing proteins from nucleic acid templates using the rules defined by the genetic code. During translation, ribosomes utilize aminoacylated tRNAs to decode mRNA codons into the corresponding polypeptide sequence. The tRNAs used in translation are aminoacylated at their 3′ ends by a family of enzymes called the aminoacyl-tRNA synthetases [aaRS[1] (1)]. The aaRSs, one of which exists for each canonical amino acid, are a highly conserved family containing two mutually exclusive structural groups, classes I and II (2-4). The high fidelity with which aaRSs match amino acids to the corresponding tRNA isoacceptors is critical for accurate translation of the genetic code.

[†]This work was supported by Grants GM22854 (D.S.) and GM65183 (M.I.) from the National Institute of General Medical Sciences.

* To whom correspondence should be addressed: Department of Microbiology, The Ohio State University, 484 W. 12th Ave., Columbus, OH 43210−1292. Phone: (614) 292−2120. Fax: (614) 292−8120. E-mail: ibba.1@osu.edu..
[‡]Ohio State Biochemistry Program, The Ohio State University.
[§]Department of Microbiology, The Ohio State University.
[‖]Tokyo Institute of Technology.
[⊥]Yale University.

[1]Abbreviations: aaRS, aminoacyl-tRNA synthetase; GluRS, glutamyl-tRNA synthetase; LysRS, lysyl-tRNA synthetase.

The need to differentiate between similar molecules within a larger cellular pool caused the synthetases to evolve precise mechanisms of substrate selection. While the catalytic mechanisms of the various aaRSs are broadly similar (5), each enzyme has developed its own method for recognizing its cognate amino acid and tRNA. For the amino acids, differentiation has been focused on recognizing differences in the size and charge of the molecules (6). To increase fidelity, several synthetases have also adopted an editing reaction to proofread misactivated noncognate amino acids (7). Errors in editing can deleteriously affect enzyme activity and lead to pathological diseases, including neurological disorders (8).

While tRNA molecules all share a basic tertiary structure that conforms to the requirements of the translation machinery (9), their diverse primary structures allow them to be more readily discriminated than amino acids. The recognition of tRNAs by synthetases is dependent on the position or modification of particular nucleotides that compose the unique identity set of each tRNA (10,11). These can be either positive determinants which enhance aminoacylation or negative determinants which prevent aminoacylation (e.g., ref 12). The identity elements of a tRNA are generally found in the acceptor stem and anticodon regions and, in a few instances, are also located in the D arm, T arm, and variable loop. The most common identity elements used are the anticodon nucleotides and the discriminator base at N73, which precedes the 3′-CCA end. By recognizing a combination of these various structural and sequential elements in tRNA, the synthetases are able to select the correct isoacceptor tRNAs with exceptional fidelity. Beyond these common features, aaRSs show divergent strategies for tRNA recognition. Most notably, the class I and class II aaRSs approach tRNAs from the minor and major groove sides of the acceptor stem, respectively (4). For most aaRSs, this difference in recognition provides an additional level at which particular tRNA isoacceptors can be differentiated. For lysyl-tRNA synthetase (LysRS), the situation is somewhat different as the enzyme is represented in both aaRS structural classes. In eukaryotes, most bacteria, and a few archaea, a class II enzyme (LysRS2) is found, whereas in some bacteria and most archaea, a class I form (LysRS1) is present (13). Aside from subtle differences in antideterminant recognition at the 2:71 base pair (14), the two forms of LysRS recognize broadly the same elements in $tRNA^{Lys}$, namely, the acceptor stem and the anticodon (15-19).

For LysRS2, anticodon recognition is mediated by the amino-terminal oligonucleotide-binding (OB) fold (20), a common motif employed by both aaRSs and other proteins that interact with RNA (21). While LysRS1 recognizes the same nucleotides as LysRS2, the anticodon is less important for tRNA identity in the class I enzyme (19). Little was known about the manner in which LysRS1 recognizes the anticodon until the crystal structure of the protein from *Pyrococcus horikoshii* was determined (22). While the crystal structure of LysRS1 with $tRNA^{Lys}$ could not be determined, the apoenzyme structure suggested the anticodon binding domain was an all-α-helix cage domain homologous to the C-terminus of *Thermus thermophilus* glutamyl-tRNA synthetase (GluRS). The α-helix cage domain comprises five or six α-helices folding into a distinctive hemispheric shape, which has been observed only in LysRS1 and eubacterial GluRS, suggesting a strong evolutionary link between the two aaRSs. On the basis of this homology, the structure of the $tRNA^{Glu}$–GluRS complex (23) was used as a template to construct a model for $tRNA^{Lys}$ binding by LysRS1 (22). From this model, a binding pocket for the anticodon was identified. To test the validity of this model and compare anticodon recognition between the different forms of LysRS, steady-state kinetics were used with variant enzymes and mutant tRNAs to examine the binding of $tRNA^{Lys}$ by LysRS1. This revealed a detailed picture of anticodon recognition by LysRS1 and also provided insights into the co-evolution of aaRSs that recognize NUY anticodon-containing tRNAs.

EXPERIMENTAL PROCEDURES

P. horikoshii LysRS1 Purification

Genes encoding the LysRS1 variants were constructed by standard methods and subcloned into the pET26b vector (Novagen) for subsequent overexpression. Wild-type *P. horikoshii* LysRS1 (22) and all variants were overexpressed in *Escherichia coli* BL21 (DE3+ RPC) cells overnight at 37 °C using Express Autoinduction System 1 (Novagen) following the manufacturer's protocol. All subsequent steps were carried out at 4 °C unless otherwise noted. Cells were harvested by centrifugation, washed, and resuspended in column buffer [50 mM HEPES (pH 7.2), 25 mM KCl, 10 mM $MgCl_2$, and 5 mM DTT]. Cells were lysed with a French pressure cell, and debris was removed by centrifugation at 45000*g* for 20 min. The resulting supernatant was flocculated at 65 °C, and floculant was removed by ultracentrifugation at 100000*g* for 1 h. The resulting solution was fractionated by FPLC using a MonoQ 5/5 column (GE Healthcare), and LysRS1 was eluted using a gradient from 0 to 500 mM NaCl in column buffer. Fractions containing LysRS1 were pooled and concentrated by ultrafiltration using an Amicon 30 filter (Millipore). The resulting solution was further purified through FPLC using a Superose 12 gel filtration column (GE Healthcare) equilibrated in column buffer. A PD-10 desalting column (GE Healthcare) was used to exchange LysRS1-containing fractions into LysRS buffer [50 mM HEPES (pH 7.2), 25 mM KCl, 10 mM $MgCl_2$, 5 mM DTT, and 10% glycerol]. The sample was again concentrated by ultrafiltration, and aliquots were then stored at −80 °C. LysRS1 was judged to be >95% pure by SDS–PAGE and Coomassie brilliant blue staining. The concentration of enzyme was determined by the Bradford assay (Bio-Rad).

$tRNA^{Lys}$ Transcription and Purification

P. horikoshii $tRNA^{Lys}$ and variants were produced and purified as previously described for *Borrelia burgdorferi* $tRNA^{Lys}$ except that NsiI replaced BstNI (24). After determination of the total RNA concentration by UV spectroscopy, the plateau of charging was found in the aminoacylation reaction to determine the percentage of active $tRNA^{Lys}$.

Aminoacylation Assays

Aminoacylation was performed at 37 °C in 100 mM HEPES (pH 7.2), 25 mM KCl, 10 mM $MgCl_2$, 4 mM DTT, 5 mM ATP, 50 μM [^{14}C]-L-Lys, and varying concentrations of LysRS1 and $tRNA^{Lys}$. Aliquots (20 μL) were taken every 30 s and spotted onto Whatman 3MM filter disks presoaked in 5% (w/v) trichloroacetic acid containing 0.5% (w/v) [^{12}C]-L-Lys. Sample disks were washed three times for 10 min at room temperature in 5% (w/v) trichloroacetic acid containing 0.5% (w/v) [^{12}C]-L-Lys and dried at 80 °C, and the level of [^{14}C]-L-Lys-$tRNA^{Lys}$ was quantified by the addition of liquid scintillant (Ultima Gold, Packard Corp.) and counting. The k_{cat}/K_M values presented here represent the average of at least three independent experiments where values deviated by no more than 15% between individual determinations.

RESULTS

The LysRS1–$tRNA^{Lys}$ Complex

The structure of the GluRS–$tRNA^{Glu}$ complex was used as a template to construct a model for the *P. horikoshii* LysRS1–$tRNA^{Lys}$ complex [Figure 1A (22)]. In the vicinity of the anticodon stem, the conformation of the α-helix cage domain of LysRS1 was altered to match the corresponding structure in the GluRS–$tRNA^{Glu}$ complex (Figure 1B). This provided a possible structure for the α-helix cage when tRNA is bound, involving both specific and nonspecific interactions. The nonspecific interactions are formed by F487 and Y491 stacking with U34 and U35, while K497 and R502 form specific hydrogen bonds with U35 and U36, respectively (Figure 2A). Analyses of the sequences of LysRS1 from various organisms support the

importance of the four residues in anticodon recognition (Figure 2B). F487 and Y491 were found to be universally conserved, while K497 (43% K, 43% Q, 8% A, 4% R, and 2% E) and R502 (69% R and 31% K) are less well-conserved. Of these, only K497 could not be replaced to produce active LysRS1 variants (data not shown). In addition to replacing the key residues, we used a series of $tRNA^{Lys}$ variants with mutated anticodons. Some of the anticodons selected were used to test the hypothesis that YUY anticodon selection could have been a cause of divergence of the class Ib synthetase enzymes, while others were selected to test the similarities and differences in anticodon recognition between LysRS1 and LysRS2.

Differentiation of Anticodon Nucleotides by Wild-Type LysRS1

For wild-type LysRS1, little difference in catalytic efficiency (k_{cat}/K_M) was observed between UUU and CUU, while the GUU variant exhibited an approximately 2-fold loss of activity (Table 1). The nucleotide at position 34 is believed to be recognized by a nonspecific stacking interaction with Phe487, consistent with comparable recognition of the UUU and CUU anticodons. The slightly reduced efficiency of the GUU substrate suggests that the size of the nucleotide may also play a role; substitution with the larger purine perhaps causes steric clashes with the amino acids of the binding site. C and G replacements at position 35 both decreased activity by a similar amount, indicating that differences in size between the purine and the pyrimidine were less important than the overall disruption of putative hydrogen bonding interactions. Significant differences were observed for the UUG and UUC mutant anticodons. UUG was discriminated at a level similar to that of UCU and UGU, while UUC exhibited a less pronounced loss of aminoacylation efficiency. The difference between C and G at position 36 may reflect the fact that either the smaller cytosine is better accommodated by the enzyme than guanosine or the extent of the disruption of the network of hydrogen bonds is smaller for cytosine than for guanosine.

Stacking Interactions with F487

The role of F487 in forming stacking interactions with U34 was investigated using an F487A LysRS1 variant (Table 2). The wild-type CUU and GUU tRNAs exhibited similar losses of aminoacylation efficiency, confirming the role of F487 in anticodon binding ($\Delta\Delta G \sim 2$ kcal/mol). The losses of aminoacylation efficiency for changes at positions 35 and 36 were additive when compared to the efficiency of the wild type (Table 2), indicating that F487 functions in the recognition of position 34.

Recognition of U35 and U36 by Y491

The ability of Y491 to form stacking interactions with U35 was investigated with the variant enzymes Y491A and Y491E (Table 3). A similar decrease in efficiency was found for the UUU, GUU, and CUU tRNAs with the Y491A variant, indicating no differentiation between the bases is taking place at position 34. For the mutant tRNAs with alterations to U35 and U36, the results were also similar to those previously obtained. All position 35 and 36 variants exhibited substantially lower catalytic efficiencies than the wild type but provided no indication of specific recognition of either position. While the model of LysRS1 with $tRNA^{Lys}$ suggested Y491 to be primarily involved in stacking with U35 (Figure 2A), it showed that it might also come close to U34. To test this placement, Y491 was mutated to Glu to examine if this altered enzyme could form new hydrogen bonds with G34 (Table 3). Most of the data obtained for the Y491E variant are nearly identical to the data for Y491A; in particular, the UUU tRNA had nearly identical k_{cat}/K_M values to GUU and CUU, indicating no differentiation of the nucleotide at position 34. The most interesting results with the variant enzyme were obtained with UUG. The k_{cat}/K_M value for this anticodon was 4 times greater than that obtained for wild-type tRNA, suggesting a substantial restoration of binding (Figure 3) and is consistent with formation of

a new hydrogen bond. This indicates that the Y491 residue, instead of fitting between U34 and U35, must stack with U35 on the opposite face bringing it close to U36.

Recognition of U36 by R502

R502 is believed to hydrogen bond with U36 in a base-specific manner. Replacement of this residue with alanine should remove the ability of the enzyme to recognize U36 specifically. As seen with the other variants, the wild-type tRNA exhibited a substantial decrease in aminoacylation efficiency with R502A, indicating an involvement of this residue in tRNA binding (Table 4). However, the loss seen for wild-type tRNA was not as large as that seen for the other variants that removed stacking interactions (Tables 2 and 3). The anticodons mutated at position 34 had k_{cat}/K_M values within the error range of UUU, indicating no specific recognition of this position. In contrast to the previous variants, UCU and UGU did not have identical losses of efficiency, with R502A twice as effective at recognizing UCU as UGU, giving some indication that this residue is involved in recognition of U35. The R502Q variant provided further evidence for the role of this residue. The original hypothesis was that if R502 formed a hydrogen bond with U36, Gln would be able to form a new bond with the UUC anticodon and rescue aminoacylation. In contrast to this expectation, all the tRNA variants exhibited substantial losses of aminoacylation efficiency. Interestingly, the effects on position 36 were significantly greater than on position 35. Taken together, these findings suggest that R502 recognizes U36, but not through hydrogen bonding interactions as originally proposed.

DISCUSSION

Remodeling of the LysRS1–tRNA^{Lys} Complex

The overall picture of anticodon binding by *P. horikoshii* LysRS1 is consistent with what was found for other LysRS1 enzymes. The enzyme recognized U35 and U36 specifically, but not U34. Some of the data also suggest that at position 36 the enzyme is more accommodating of cytosine than of guanosine replacements. The anticodon did not appear to be as crucial for recognition as in other aaRSs, with losses of aminoacylation efficiency only ~1−2 orders of magnitude. LysRS2, which also uses the anticodon for recognition, showed losses of aminoacylation efficiency 2−4 orders of magnitude or greater upon replacement of several of the same anticodon nucleotides investigated here (20). In an attempt to better understand these differences in the apparent importance of anticodon recognition between class I and class II LysRSs, the interactions between LysRS1 and the region from nucleotides 30−40 of tRNA^{Lys} were remodeled on the basis of the biochemical data described above (Figure 4). In this model, the side chain of R502 is shifted and makes a tighter contact with U36 than originally proposed, thereby explaining the inability of the R502Q variant to rescue aminoacylation of the UUC anticodon which had been expected from the previous model (Figure 2A). In this revised model, F487 stacks with U34 and Y491 stacks with U35, in agreement with the biochemical data. However, it is impossible for Y491 to directly interact with U36 in this or any other reasonable orientation, suggesting additional conformational changes upon complex formation, which will be clarified only upon determination of the LysRS1–tRNA^{Lys} cocrystal structure. The availability of this structure would also help to clarify whether both LysRS1 and LysRS2 are able to simultaneously recognize the anticodon during formation of a ternary complex with tRNA^{Lys} (25), or if instead only one of the synthetases binds the anticodon. While the picture of exactly how LysRS1 recognizes the anticodon remains incomplete, it is clear that considerably fewer stacking and hydrogen bonding interactions are involved in binding this region of tRNA^{Lys} than in LysRS2 (20,26), providing a structural basis for the diminished dependence on anticodon recognition for the class I compared to the class II enzyme.

Differentiation of NUY Anticodon tRNAs by LysRS1 and GluRS

Structural and phylogenetic studies indicate that LysRS1 may have evolved from an ancestral GluRS (23,27). This study supports this suggestion and provides insights into the possible evolution of tRNA specificity in LysRS1 originating from an enzyme perhaps similar to one of the contemporary nondiscriminating GluRSs (ndGluRS) that are able to recognize YUY/G anticodons. GluRS and LysRS1 are both class Ib aaRSs that recognize YUY anticodons using the same RNA binding domain architecture. LysRS1 is essentially indifferent to the first position of the anticodon (Table 1), in contrast to LysRS2, which shows some discrimination of this position (20). In the absence of differentiation of the nucleotide at position 34, the only necessary change in tRNA recognition for LysRS1 compared to an ndGluRS is the ability to discriminate U from C/G at position 36. For example, in *T. thermophilus*, GluRS R358 is responsible for recognition of C at position 36 in $tRNA^{Glu}$, and replacement of this position with Gln is sufficient to accommodate the UUG anticodon (23). *P. horikoshii* LysRS1 R502 plays a somewhat analogous role, but in this case, recognition is more stringent since changes of this residue do not accommodate changes at the third position of the anticodon (Table 4). Instead, the specificity of recognition of U36 is at least in part determined by interactions with Y491 (Table 3 and Figure 3), but no potentially comparable interactions have been seen during anticodon recognition by GluRS. Taken together with previous studies of GluRS, the data presented here indicate how specificity for the anticodon of $tRNA^{Lys}$ could have been acquired through relatively few changes in the α-helix cage RNA binding domain of an ancestral GluRS enzyme.

ACKNOWLEDGMENT

We thank C. Hausmann, J. Ling, and T. Rogers for critical reading of the manuscript.

REFERENCES

1. Ibba M, Söll D. Aminoacyl-tRNA synthesis. Annu. Rev. Biochem 2000;69:617–650. [PubMed: 10966471]
2. Eriani G, Delarue M, Poch O, Gangloff J, Moras D. Partition of tRNA synthetases into two classes based on mutually exclusive sets of sequence motifs. Nature 1990;347:203–206. [PubMed: 2203971]
3. Cusack S, Berthet-Colominas C, Hartlein M, Nassar N, Leberman R. A second class of synthetase structure revealed by X-ray analysis of *Escherichia coli* seryl-tRNA synthetase at 2.5 Å. Nature 1990;347:249–255. [PubMed: 2205803]
4. Ribas De Pouplana L, Schimmel P. Two classes of tRNA synthetases suggested by sterically compatible dockings on tRNA acceptor stem. Cell 2001;104:191–193. [PubMed: 11269237]
5. Zhang CM, Perona JJ, Ryu K, Francklyn C, Hou YM. Distinct kinetic mechanisms of the two classes of aminoacyl-tRNA synthetases. J. Mol. Biol 2006;361:300–311. [PubMed: 16843487]
6. Ataide SF, Ibba M. Small molecules: Big players in the evolution of protein synthesis. ACS Chem. Biol 2006;1:285–297. [PubMed: 17163757]
7. Hendrickson, TL.; Schimmel, P. Translation Mechanisms. Lapointe, J.; Brakier-Gingras, L., editors. Kluwer Academic/Plenum Publishers, Dordrecht, The Netherlands; 2003. p. 34-64.
8. Lee JW, Beebe K, Nangle LA, Jang J, Longo-Guess CM, Cook SA, Davisson MT, Sundberg JP, Schimmel P, Ackerman SL. Editing-defective tRNA synthetase causes protein misfolding and neurodegeneration. Nature 2006;443:50–55. [PubMed: 16906134]
9. Dale T, Uhlenbeck OC. Amino acid specificity in translation. Trends Biochem. Sci 2005;30:659–665. [PubMed: 16260144]
10. Giegé R, Puglisi JD, Florentz C. tRNA structure and aminoacylation efficiency. Prog. Nucleic Acid Res. Mol. Biol 1993;45:129–206. [PubMed: 8341800]
11. Giegé R, Sissler M, Florentz C. Universal rules and idiosyncratic features in tRNA identity. Nucleic Acids Res 1998;26:5017–5035. [PubMed: 9801296]

12. Fukunaga R, Yokoyama S. Aminoacylation complex structures of leucyl-tRNA synthetase and $tRNA^{Leu}$ reveal two modes of discriminator-base recognition. Nat. Struct. Mol. Biol 2005;12:915–922. [PubMed: 16155584]
13. Ambrogelly A, Korencic D, Ibba M. Functional annotation of class I lysyl-tRNA synthetase phylogeny indicates a limited role for gene transfer. J. Bacteriol 2002;184:4594–4600. [PubMed: 12142429]
14. Ibba M, Losey HC, Kawarabayasi Y, Kikuchi H, Bunjun S, Söll D. Substrate recognition by class I lysyltRNA synthetases: A molecular basis for gene displacement. Proc. Natl. Acad. Sci. U.S.A 1999;96:418–423. [PubMed: 9892648]
15. Tamura K, Himeno H, Asahara H, Hasegawa T, Shimizu M. In vitro study of *E. coli* $tRNA^{Arg}$ and $tRNA^{Lys}$ identity elements. Nucleic Acids Res 1992;20:2335–2339. [PubMed: 1375736]
16. Commans S, Plateau P, Blanquet S, Dardel F. Solution structure of the anticodon-binding domain of *Escherichia coli* lysyl-tRNA synthetase and studies of its interaction with $tRNA^{Lys}$. J. Mol. Biol 1995;253:100–113. [PubMed: 7473706]
17. Shiba K, Stello T, Motegi H, Noda T, Musier-Forsyth K, Schimmel P. Human lysyl-tRNA synthetase accepts nucleotide 73 variants and rescues *Escherichia coli* double-defective mutant. J. Biol. Chem 1997;272:22809–22816. [PubMed: 9278442]
18. Söll D, Becker HD, Plateau P, Blanquet S, Ibba M. Context-dependent anticodon recognition by class I lysyl-tRNA synthetases. Proc. Natl. Acad. Sci. U.S.A 2000;97:14224–14228. [PubMed: 11121028]
19. Ambrogelly A, Frugier M, Ibba M, Söll D, Giegé R. Transfer RNA recognition by class I lysyl-tRNA synthetase from the Lyme disease pathogen *Borrelia burgdorferi*. FEBS Lett 2005;579:2629–2634. [PubMed: 15862301]
20. Commans S, Lazard M, Delort F, Blanquet S, Plateau P. tRNA anticodon recognition and specification within subclass IIb aminoacyl-tRNA synthetases. J. Mol. Biol 1998;278:801–813. [PubMed: 9614943]
21. Theobald DL, Wuttke DS. Divergent evolution within protein superfolds inferred from profile-based phylogenetics. J. Mol. Biol 2005;354:722–737. [PubMed: 16266719]
22. Terada T, Nureki O, Ishitani R, Ambrogelly A, Ibba M, Söll D, Yokoyama S. Functional convergence of two lysyl-tRNA synthetases with unrelated topologies. Nat. Struct. Biol 2002;9:257–262. [PubMed: 11887185]
23. Sekine S, Nureki O, Shimada A, Vassylyev DG, Yokoyama S. Structural basis for anticodon recognition by discriminating glutamyl-tRNA synthetase. Nat. Struct. Biol 2001;8:203–206. [PubMed: 11224561]
24. Levengood J, Ataide SF, Roy H, Ibba M. Divergence in noncognate amino acid recognition between class I and class II lysyl-tRNA synthetases. J. Biol. Chem 2004;279:17707–17714. [PubMed: 14747465]
25. Polycarpo C, Ambrogelly A, Ruan B, Tumbula-Hansen D, Ataide SF, Ishitani R, Yokoyama S, Nureki O, Ibba M, Söll D. Activation of the pyrrolysine suppressor tRNA requires formation of a ternary complex with class I and class II lysyl-tRNA synthetases. Mol. Cell 2003;12:287–294. [PubMed: 14536069]
26. Cusack S, Yaremchuk A, Tukalo M. The crystal structures of *T. thermophilus* lysyl-tRNA synthetase complexed with *E. coli* $tRNA^{Lys}$ and a *T. thermophilus* $tRNA^{Lys}$ transcript: Anticodon recognition and conformational changes upon binding of a lysyl-adenylate analogue. EMBO J 1996;15:6321–6334. [PubMed: 8947055]
27. Salazar JC, Ahel I, Orellana O, Tumbula-Hansen D, Krieger R, Daniels L, Söll D. Coevolution of an aminoacyl-tRNA synthetase with its tRNA substrates. Proc. Natl. Acad. Sci. U.S.A 2003;100:13863–13868. [PubMed: 14615592]

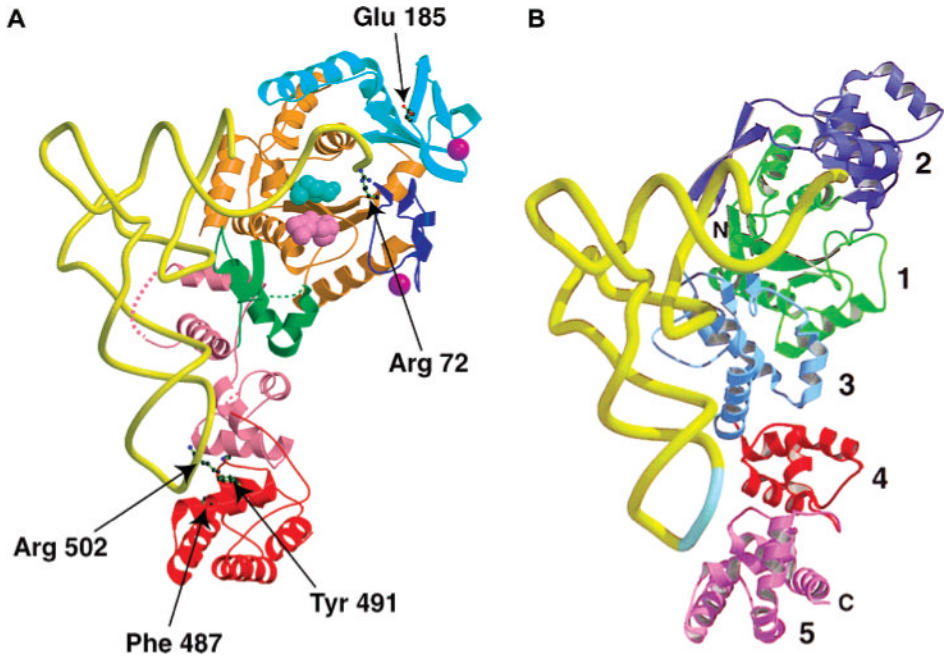

Figure 1.

Comparison of LysRS1 and GluRS structures. (A) Model of the LysRS1–tRNA^{Lys} complex. The Rossman fold is colored orange, while the α-helix cage domain is colored red. Some of the residues involved in tRNA recognition are labeled. Adapted from ref 22. (B) Structure of the GluRS–tRNA^{Glu} complex. Crystal structure of GluRS with tRNA^{Glu} bound. The Rossman fold is colored green, while the α-helix cage domain, which is homologous to the one in LysRS1, is colored purple. The tRNA is colored yellow with the anticodon colored gray. Adapted from ref 23.

A

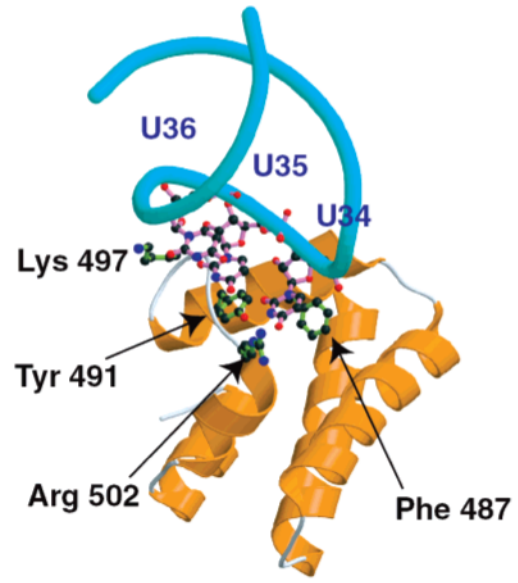

B

```
                481                                   521
P. horikoshii   ISSREWFSTLYRLFIGKERGPRLASFLASLDRSFVIKRLRL
B. burgdorferi  IEPALFFKQIYKILIDKEKGPKLAGFIKGIDRFEKITSKYV
F. acidarmanus  LTPKDVFTLFYRVFIDKDKGPRLGYFLSSMDKNYVVNRIKS
M. jannaschii   LNPRDAFQASYMILLGKKYGPKLGAFLATLGKDFVIRRYSL
M. barkeri      VDPRELFKAIYISLLGQSSGPKAGWFLSSFEKEFLVERFEE
M. maripaludis  LAPKEAFVASYKILLGKNYGPKLGSFLASLKKEFVIGRFNL
```

Figure 2.

tRNA^{Lys} anticodon binding by LysRS1. (A) Detail of the amino acid residues believed to interact with the anticodon nucleotides (adapted from ref 22). (B) Sequence alignments of selected LysRS1 species highlighting conservation of residues in the anticodon binding domain. Residues believed to recognize the anticodon are underlined.

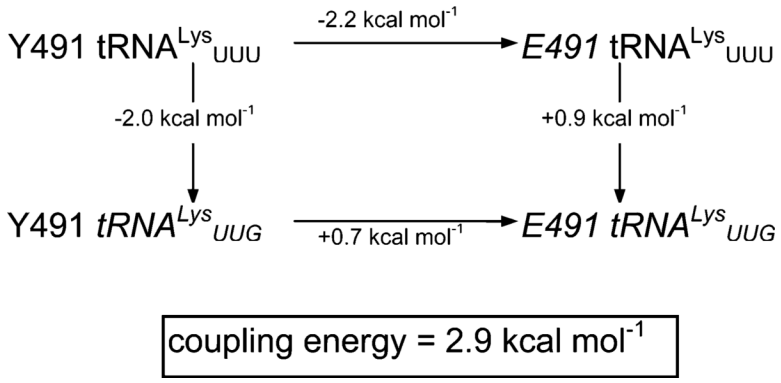

Figure 3.
Double mutant cycle analysis for LysRS1 Y491E aminoacylation of tRNA^{Lys} UUG.

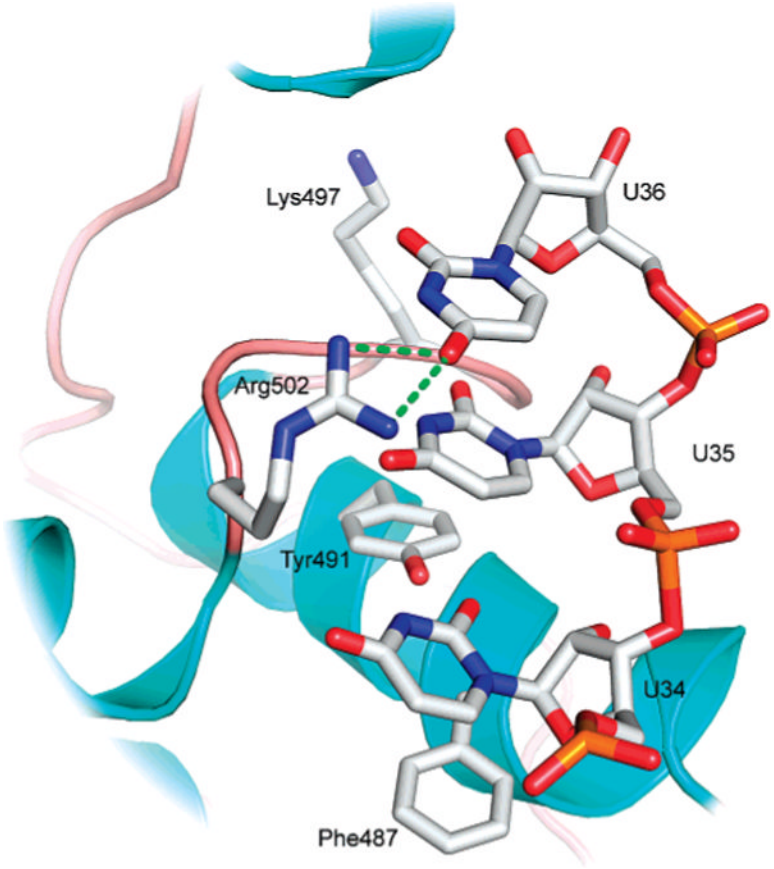

Figure 4.
Model for $tRNA^{Lys}$ anticodon binding by *P. horikoshii* LysRS1. Molecular modeling of the LysRS1–tRNA complex was accomplished with O. Adjustments were made manually on the basis of the results from mutation of $tRNA^{Lys}$ and LysRS1. The conformational changes were reminiscent of those previously observed in the GluRS–$tRNA^{Glu}$ complex.

Table 1

Kinetic Data for Wild-Type LysRS1 with Mutant tRNAs

$tRNA^{Lys}$ ($N_{34}N_{35}N_{36}$)	K_M(μM)	k_{cat}(s^{-1})	k_{cat}/K_M($s^{-1}\mu M^{-1}$)	L^a
UUU	0.87 ± 0.09	0.044 ± 0.002	0.051 ± 0.01	1
CUU	1.4 ± 0.2	0.062 ± 0.004	0.044 ± 0.05	1.2
GUU	1.5 ± 0.01	0.043 ± 0.0001	0.029 ± 0.0003	1.8
UCU			0.0019 ± 0.00008[b]	27
UGU			0.0017 ± 0.0001	30
UUC			0.0035 ± 0.0002	15
UUG			0.0021 ± 0.00006	24

[a] The aminoacylation efficiency of each enzyme—tRNA pair was compared to that of the wild-type enzyme with wild-type tRNA. A value, *L*, was found as the loss of aminoacylation efficiency $[k_{cat}(wt)/K_M(wt)]/[k_{cat}(mut)/K_M(mut)]$.

[b] For $tRNA^{Lys}$ variants containing changes at positions 35 and 36, tRNA could not be used at saturating concentrations because of the high K_M compared to practical tRNA concentrations. When [S] << K_M, k_{cat}/K_M was directly estimated from the equation $v = k_{cat}/K_M([E][S])$.

Table 2

Kinetic Data for LysRS1 Variant F487A with Mutant tRNAs

tRNA ($N_{34}N_{35}N_{36}$)	k_{cat}/K_M ($s^{-1}\mu M^{-1}$)	L	M^a
UUU	0.0019 ± 0.00006	27	1
CUU	0.0027 ± 0.0001	19	0.7
GUU	0.0022 ± 0.0002	23	0.9
UCU	0.00099 ± 0.00006	52	1.9
UGU	0.00087 ± 0.00006	59	2.2
UUC	0.0015 ± 0.0001	34	1.3
UUG	0.0010 ± 0.00006	49	1.8

[a] k_{cat}/K_M for the variant enzyme with the wild-type tRNA was set to 1, and each mutant tRNA was then compared to this to give a value M.

Table 3

Kinetic Data for LysRS1 Y491 Variants with Mutant tRNAs

tRNA ($N_{34}N_{35}N_{36}$)	k_{cat}/K_M ($s^{-1}\mu M^{-1}$)	*L*	*M*
Y491A			
UUU	0.0016 ± 0.00007	32	1
CUU	0.0017 ± 0.00009	30	0.9
GUU	0.0015 ± 0.0001	34	1.1
UCU	0.00079 ± 0.00009	65	2.0
UGU	0.00076 ± 0.00003	67	2.1
UUC	0.0010 ± 0.00007	51	1.6
UUG	0.00090 ± 0.000005	57	1.8
Y491E			
UUU	0.0015 ± 0.00007	34	1
CUU	0.0014 ± 0.00008	36	1.1
GUU	0.0015 ± 0.0001	34	1
UCU	0.00094 ± 0.00006	54	1.6
UGU	0.00087 ± 0.00007	59	1.7
UUC	0.0013 ± 0.0001	39	1.2
UUG	0.0064 ± 0.0004	8	0.2

Table 4

Kinetic Data for LysRS1 R502 Variants with Mutant tRNAs

tRNA ($N_{34}N_{35}N_{36}$)	k_{cat}/K_M ($s^{-1}\mu M^{-1}$)	*L*	*M*
R502A			
UUU	0.0029 ± 0.0002	18	1
GUU	0.0031 ± 0.0001	16	0.9
CUU	0.0032 ± 0.0001	16	0.9
UCU	0.0013 ± 0.00007	39	2.2
UGU	0.00079 ± 0.00003	65	3.7
UUC	0.0007 ± 0.00006	73	4.1
UUG	0.00085 ± 0.00005	60	3.4
R502Q			
UUU	0.00057 ± 0.00003	89	1
GUU	0.00053 ± 0.000006	96	1.1
CUU	0.00055 ± 0.00003	93	1.0
UCU	0.00018 ± 0.00001	280	3.2
UGU	0.00018 ± 0.0000007	280	3.2
UUC	0.000073 ± 0.000007	700	7.8
UUG	0.000078 ± 0.000004	650	7.3